Assessing structural integrity of non-homogeneous systems by means of Acoustic Emissions and Non-Extensive Statistical Mechanics

Stavros K. Kourkoulis, Ermioni D. Pasiou
National Technical University of Athens, School of Applied Mathematical and Physical Sciences, Department of Mechanics, Laboratory for Testing and Materials, 5, Heroes of Polytechneion Avenue, "Pericles Theocaris" Building, Zografou Campus, 157 73, Zografou, Attiki, Greece
stakkour@central.ntua.gr, http://orcid.org/0000-0003-3246-9308
epasiou@central.ntua.gr, http://orcid.org/0000-0003-1580-3415

Ilias Stavrakas, Dimos Triantis
University of West Attica, Faculty of Engineering, Department of Electrical and Electronics Engineering, Electronic Devices and Materials Laboratory, Ancient Olive Grove Campus, Building B, 250 Thivon Avenue, Egaleo Postal Code 122 44, Athens, Greece
ilias@uniwa.gr, http://orcid.org/0000-0001-8484-8751
triantis@uniwa.gr, http://orcid.org/0000-0003-4219-8687

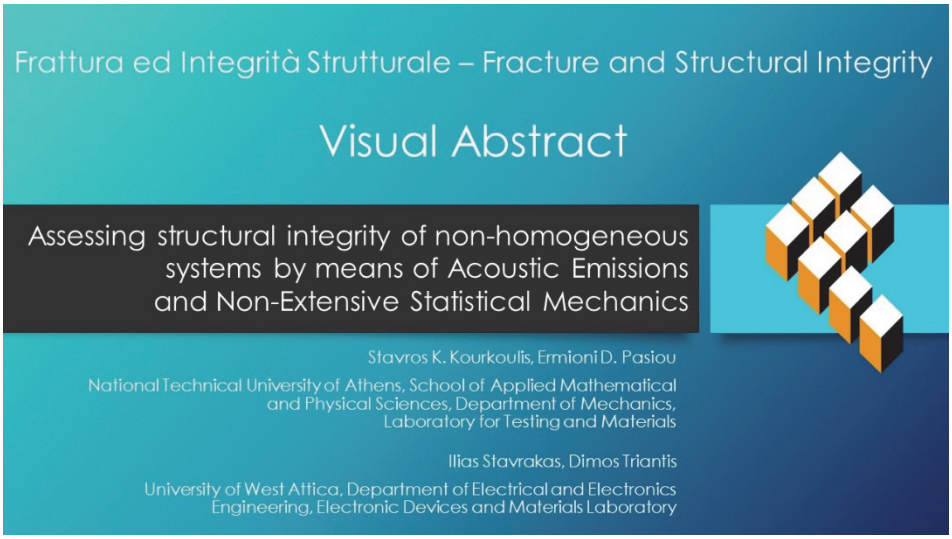

Citation: Kourkoulis, S.K., Pasiou, E.D., Stavrakas, I., Triantis, D., Assessing structural integrity of non-homogeneous systems by means of Acoustic Emissions and Non-Extensive Statistical Mechanics, Frattura ed Integrità Strutturale, 68 (2024) 440-457.

Received: 29.02.2024
Accepted: 26.03.2024
Published: 28.03.2024
Issue: 04.2024

KEYWORDS. Structural Integrity, Structural Health Monitoring, Interevent times, Pre-failure indices, Non-Extensive Statistical Mechanics, Non-additive entropies.

INTRODUCTION

Quantifying the level of damage at the interior of a mechanically loaded system (either it is a specimen in the laboratory scale or a structure/structural element in the field), is among the issues that seriously concern the community of Structural Engineers, since it is inextricably linked to the system's load carrying capacity and its structural integrity. The field developed to confront this issue, i.e., that of Structural Health Monitoring (SHM), is growing explosively worldwide and the technique mainly employed is that of the Acoustic Emissions (AE), the most mature and firmly founded one. Nowadays, the acoustic activity generated in a loaded structure is analyzed by means of a wide series of parameters (or combinations of parameters) including the production rate of acoustic hits or events, the cumulative counts, the rise time (or the rise time over the respective amplitude (RA)) of the acoustic hits, their average frequency (AF), the relation between RA and AF, the energy or the power of the acoustic hits, the b-values, the interevent time (IT) between successive acoustic hits or events, the distance (Euclidean) between the sources of successive acoustic events etc.

An alternative approach for the exploitation of experimental data related to the acoustic activity was introduced recently, based on the theory of Non-Extensive Statistical Mechanics (NESM), a scientific discipline on the boundary between Mechanics and Physics. The principal characteristic of NESM is that it is developed in terms of a new class of entropies which violate the principle of additivity, the cornerstone of the traditional Boltzmann-Gibbs Statistical Mechanics (BGSM). A series of non-additive entropies have been introduced, however, the one that is nowadays most widely adopted is the S_q entropy, which was proposed about thirty-five years ago by Tsallis [1]. S_q has been employed successfully for the analysis of problems in a broad variety of disciplines either in laboratory [2, 3] or in-field scales (ranging from Strength of Materials, Seismology, and Earthquake Engineering [4] to Finance, Medicine and Social Sciences [5]).

The concepts of NESM were recently applied in the direction of detecting pre-failure indices while brittle building materials (like marble and concrete) are submitted to mechanical loading schemes, including direct tension, three-point bending, compression, and diametral compression etc. [6]. Interesting conclusions were drawn from the temporal evolution of the entropic index q, namely the factor that quantifies the degree of non-additivity of a system according to the founding principles of NESM and the definition of S_q. More specifically it was highlighted that during loading the entropic index increases, moving gradually away from the limiting value of q=1 (the limit for which Tsallis entropy degenerates to the Boltzmann-Gibbs one). According to NESM, significant deviations of q from unity is attributed to well-organized processes of generation and development of networks of micro-cracks. Moreover, it was concluded that slightly before the applied load reaches its maximum value, q tends towards a global maximum around $q\approx1.40$ (the exact value depends on the loading scheme and the material) and then it starts decreasing towards the q=1 limit. According to existing data [7], this tendency of q to re-approach the limiting value of q=1, is an indication that mechanisms leading to intense generation of macro-cracks are activated, leading eventually to fatal propagation of these macro-cracks and to macroscopic fracture.

Besides materials of almost "perfect" homogeneity like marble, materials with a certain degree of inhomogeneity (fiber-reinforced concrete) were tested in that study [6] and, also, in a recently published one [8]. It is interesting to note that for these materials instead of a global maximum the temporal evolution of q at the very last loading stages was characterized by a global minimum which was attributed to the activation of an additional damage mechanism (which does not appear in homogeneous materials), namely the debonding between the concrete mass and the reinforcing fibers.

In this context, an attempt is described here to study the acoustic activity developed in strongly non-homogeneous systems consisting of different materials. As a typical example, restored structural elements of the Temple of Parthenon on the Athenian Acropolis were considered. The specimens prepared for the experimental protocol simulated either fragmented epistyles restored by means of threaded bars of titanium and suitable cementitious material or blocks of marble which were mutually interconnected using "I"- or "ΙΤ"-shaped connectors made from titanium. The restored epistyles were subjected to bending while the interconnected marble blocks to a pure shear loading scheme.

The acoustic activity developed in both cases was analyzed in terms of the IT intervals between any two successive acoustic events. Proper elaboration of the experimental data provided the temporal evolution of the entropic index q, which was considered in juxtaposition to the respective evolution of the applied load as well as to the average frequency of generation of acoustic events. It was indicated that the response of these complexes (which are characterized by the multiplicity of materials and the existence of macroscopically visible interfaces) is more complicated if compared to the respective one of specimens of macroscopically homogenous nature (like, for example, those made of fiber-reinforced concrete). However, interesting qualitative similarities were revealed. Indeed, q attains high numerical values from relatively early loading stages, reflecting the existence of mutually interacting systems due to the geometry and the multiplicity of materials, suggesting that the acoustic activity is more efficient to be analyzed in terms of NESM rather than of BGSM. Again, it is the existence of a global minimum (or minima) that designates entrance to criticality (i.e., stage of impending fracture), contrary to what was observed for specimens made of materials with "perfect" homogeneity (at least from the macroscopic point of view).

THEORETICAL PRELIMINARIES: BASIC CONCEPTS OF NON-EXTENSIVE STATISTICAL MECHANICS

The word *entropy* (emanating from the Greek words *εν+τρέπω,* i.e., *in+transform/change*) was introduced by Clausius [9], who stated that *"Every bodily system possesses in every state a particular entropy, and this entropy designates the preference of nature for the state in question; in all the processes which occur in the system, entropy can only grow, never diminish"* [10]. Although Clausius did not define *what entropy is*, it could be deduced that entropy was inseparably connected to an unavoidable degradation of energy from a usable form into an unusable one. Later on, Maxwell indicated that the "*entropy had to be a distinct physical property of a body and must be zero when completely deprived of heat*" [11]. In other words, while heat transfer takes place in a system of bodies, the entropy of the system increases.

In general, the idea persisting was that the absolute value of entropy cannot be determined (measured) and only its changes were determinable ("*The entropy, like the energy, is, therefore, determinable only as regards its changes and not in absolute value*" [12]). The impossibility of determining the absolute value of entropy was opposed by Boltzmann, Gibbs and Planck, who proposed a more detailed microscopic description of the concept [13], as:

$$S_B = -k\sum_{i=1}^{W} p_i \ln p_i \tag{1}$$

In Eqn.(1) W represents the overall number of (microscopic) configurations (a measure of disorder), p_i are the probabilities corresponding to the above mentioned configurations (summing up to 1), and k is the familiar Boltzmann's constant (connecting macroscopic thermodynamics to the microscopic perspective of Boltzmann/Gibbs/Planck). In case of equality of the probabilities (i.e., $p_i=1/W, \forall i$), one obtains the familiar equation defining the so-called Boltzmann-Gibbs entropy, S_{BG}:

$$S_{BG} = k \ln W \tag{2}$$

Eqs.(1, 2) reflect a fundamental issue of Physics, suggesting that the 2nd law of thermodynamics must be considered as an interconnection between probability and entropy and, therefore, its nature is purely statistical. Although at that era the microscopic perspective of entropy was not accepted "smoothly" by the scientific community (even Einstein was sceptic [14]), it became gradually one of the monumental pillars of Physics, and it has been applied successfully for more than a century, providing answers to numerous problems of Physics and Mechanics.

BGSM is based on a series of simplifications (as it is, for example, ergodicity), which are well-acceptable for systems in which "*…microscopic variables behave, from the probabilistic viewpoint, as (nearly) independent*" [15]. However, it is well known that "*…phenomena exist, in natural, artificial and social systems (geophysics, astrophysics, biophysics, economics, and others) that violate ergodicity. To cover a (possibly) wide class of such systems, a generalization … of the BG theory was proposed in 1988… based on nonadditive entropies*" [15]. Among nonadditive entropies the one most widely used nowadays in the discipline of Mechanics is Tsallis entropy, which will be noted from here on as S_q. Assuming that a given variable X, for which the occurrence of any value X_i is described by the probability distribution p_i, S_q is calculated as [1]:

$$S_q = \frac{k}{q-1}\left(1-\sum_{i=1}^{w} p_i^q\right) \tag{3}$$

where q denotes the "*entropic index*", which is considered as a measure of the degree of non-additivity of the system. Indeed, for two subsystems I and II, it is concluded from Eqn.(3) that:

$$S_q(I+II) = S_q(I) + S_q(II) + \frac{1-q}{k} S_q(I) S_q(II) \tag{4}$$

clearly reflecting the system's non-additivity. q-values exceeding unity correspond to systems with sub-additivity, i.e., $S_q(I+II)<S_q(I)+S_q(II)$. On the contrary, q-values which are smaller than unity correspond to systems with super-additivity, i.e., $S_q(I+II)>S_q(I)+S_q(II)$. In addition, q is a measure of the non-extensivity of a system composed of non-independent subsystems, which exhibit memory effects and, in addition, they are characterized by long-range interactions. In this context, q is assumed to somehow reflect the system's multi-fractality.

It is nowadays accepted that systems with q deviating from unity are characterized by organized processes which are responsible for the generation and development of networks of micro-cracks. On the other hand, systems described by q-values

close to unity are characterized by processes of intense generation and propagation of macro-cracks leading, eventually, to fatal disintegration [7].
While dealing with Tsallis entropy it is convenient to employ the Cumulative Distribution Function (CDF) of the variable X. CDF is expressed in terms of the q-exponential function, $\exp_q(X)$, which is usually written as (see for example ref.[16]):

$$P(>X)=\exp_q\left(-\beta_q X\right) \tag{5}$$

where $\exp_q(X)$ is defined as follows:

$$\exp_q(X)=\begin{cases}\left(1+X-qX\right)^{\frac{1}{1-q}}, & \left(1+X-qX\right)\geq 0\\ 0, & \left(1+X-qX\right)\leq 0\end{cases} \tag{6}$$

In Eqn.(5) β_q is an entropic parameter, depending on the nature of the system studied. Clearly, in case $q\rightarrow 1$, then $\exp_q(X)$ becomes the well-known exponential function.

THE PROCEDURE TO EXPLORE THE ACOUSTIC ACTIVITY USING THE IT INTERVALS AND NESM

To explore the acoustic activity developed in composite marble specimens (which simulate structural members of the Parthenon Temple) under various loading schemes (described analytically in next section), the temporal evolution of parameters defined by means of the NESM will be considered in this study. To achieve this target, time series of acoustic events which were recorded during the experimental procedure, were analyzed in terms of the IT intervals [17] between any two successive acoustic events, $\delta\tau_i$, defined as:

$$\delta\tau_i=t_{i+1}-t_i \tag{7}$$

In Eqn.(7) t_i, t_{i+1} correspond, respectively, to the time instants at which the i^{th} and the $(i+1)^{th}$ events were recorded. Considering $\delta\tau$ as the X parameter of Eqn.(5), it has been proven experimentally [3, 16, 18, 19] that the CDF of the IT intervals obeys a q-exponential function into the form of:

$$P(>\delta\tau)=\exp_q\left(-\beta_q\cdot\delta\tau\right)=\left[1+(q-1)\beta_q\cdot\delta\tau\right]^{\frac{1}{1-q}} \tag{8}$$

In Eqn.(8) the entropic parameter β_q is defined as $\beta_q=1/\tau_q$. Its unit is that of inverse time (s^{-1}), and τ_q is related to the average value $\overline{\delta\tau}$ of the group of IT intervals used for the determination of their CDF $P(>\delta\tau)$, through the relation [16]:

$$\frac{\overline{\delta\tau}}{\tau_q}=B\left(2,\frac{2-q}{q-1}\right)\cdot(q-1)^{-2} \tag{9}$$

In Eqn.(9) B(x,y) denotes the familiar Beta function determined as [20]:

$$B(x,y)=\int_0^1\frac{t^{x-1}}{(1-t)^{1-y}}dt,\quad \text{with } x=2 \text{ and } y=\frac{2-q}{q-1} \tag{10}$$

The procedure adopted in order to describe the temporal evolution of the entropic index q and that of the entropic parameter β_q, is shortly outlined as follows:

- The acoustic events that were recorded during the whole loading procedure are divided into a number of k sub-groups, assuming a certain degree of overlapping among any two successive groups, as it will be explained below. The numerical value of k depends mainly on the total number of acoustic events that were recorded in each test.
- As a second step, the IT intervals $\delta\tau$ of the AE events of each group are determined.
- Then, the respective CDF $P(>\delta\tau)$ is plotted versus $\delta\tau$ for all the k groups of acoustic events.

- Finally, curve fitting (in terms of the differential evolution algorithm [21]), provides the numerical values of q and β_q.
- In addition, for each group of AE events, the mean value of the load applied is, also, calculated.

In Fig.1 a typical example is considered highlighting the above-described procedure for the determination of q and β_q. In this figure the CDF P(>δτ) (as it was determined for the first group of acoustic events of a typical test of the experimental protocol with shear loading of mutually interconnected marble epistyles) is plotted versus the IT interval δτ, and it is fitted by means of Eqn.(8). It is seen that, excluding a very short 'tail' at the end of the plot, Eqn.(8) fits excellently the experimental data, providing numerical values for q and β_q equal to 1.50 and 1.69 s^{-1}, respectively.

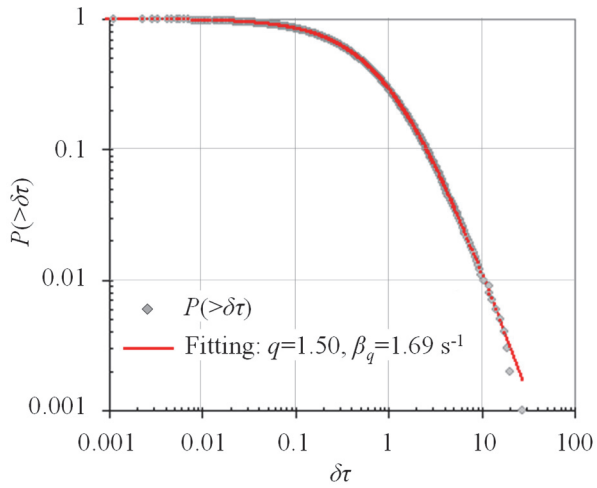

Figure 1: The CDF P(>δτ) for a given group of experimentally determined IT intervals plotted versus the IT intervals, together with the respective fitting curve according to Eqn.(8).

EXPERIMENTAL PROTOCOLS: MATERIALS, SPECIMENS AND THEIR MECHANICAL RESPONSE

All monuments of the Athenian Acropolis were constructed from Pentelic marble, a mountain in the Attika region, Greece. Considering that nowadays the exploitation of the specific quarries is not permitted (for environmental and cultural heritage protection reasons), the need for marble of the restoration project of the monuments of the Acropolis hill (in progress since 1981) are covered using Dionysos marble, the mechanical response of which is quite similar (if not identical) to that of the Pentelic marble. A synoptic description of the mechanical and physical properties of Dionysos marble can be found in earlier publications [22, 23].

The specimens of all three protocols that will be discussed in this study were carefully designed and prepared by the experienced personnel of the Acropolis work site, in strict accordance with a pioneering restoration technique that has been developed by the scientific team working for the Acropolis restoration project. According to the specific technique, the restoration of damaged structural elements (and, also, the interconnection of independent structural members) is achieved using titanium connectors of various shapes, which are placed in holes or grooves (drilled or sculptured on the marble elements), which are then filled by a proper cementitious material. The reasoning behind these decisions and technical details concerning the practical application of the specific technique are analytically described in a series of milestone works (see, for example, refs. [22, 24, 25]).

The above procedure results in complexes consisting of three elements (marble-titanium-cement paste) and three interfaces, namely, marble-to-cement paste, cement paste-to-titanium and marble-to-marble. The analysis of the mechanical behaviour of these complexes is quite challenging from the engineering point of view (and the same is true for their Structural Health Monitoring) since any damage mechanism is first activated at the above-mentioned interfaces and, therefore, information is required from the interior of the restored complexes. Analysis of the acoustic activity generated during mechanical loading of these restored elements is proven to be the most reliable tool that could offer a solution to the problem.

Bending of an asymmetrically fractured and restored epistyle

In this protocol, a copy of a typical epistyle of the Parthenon (at a scale of 1:3) was tested. It consisted of two asymmetric fragments (of trapezoidal profile), joined together by means of three pairs of bolted titanium bars of diameter 8 mm (threaded all along their length), which were driven in pre-drilled holes that were filled with liquid cement paste (as it is seen

in Fig.2a, in which the two fragments are shown while they are brought into mutual contact). The dimensions of the specimen and the position of three pairs of bars can be seen in Fig.2b. The anchoring length was 25 cm on either side of the fracture plane. The specimen was cured for one month. Afterwards, it was tested under ten-point bending by means of eight metallic rollers (and an improvised system of wide flange H-beams) and two marble cubes which simulated the capitals on which the epistyles rest in the actual conditions at the Parthenon Temple. A stiff servo-hydraulic frame (AMSLER, 6 MN) was used to load the specimen. Its capacity was equal to 6 MN. The loading procedure was monotonic until the fracture of the epistyle. Displacement-controlled conditions were adopted, at a constant rate equal to about 0.3 mm/min. A photo of the specimen just after the fracture of the reinforcing titanium bars is shown in Fig.2c.
For the detection and recording of the acoustic activity eight acoustic sensors (R15α, Mistras Group, Inc., New Jersey, USA) were used, properly attached at strategic points of the "epistyle" at either side of the interface of the two fragments. The displacements developed during loading were monitored using a 3D-Digital Image Correlation (DIC) system (LIMESS, Messtechnik & Software GmbH, Germany).

(a)

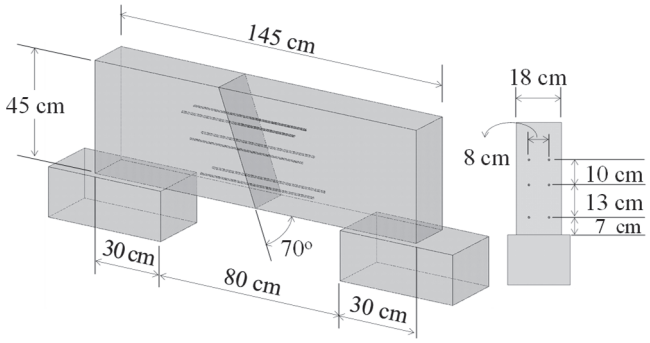

(b)

(c)

Figure 2: (a) The two fragments of the epistyle while brought in contact; (b) A sketch indicating the dimensions of the restored epistyle; (c) The epistyle after it was tested [26].

In Fig.3a the applied load is plotted against the displacement (deflection of the epistyle's central section), while in Fig.3b the temporal evolution of the distance between the two fragments (at the bottom line of the epistyle and, also, at the levels of the two lower pairs of reinforcing bars) is plotted as it was obtained by the DIC system.
Comparative consideration of the two figures reveals that the specific experiment can be divided into four, clearly distinguishable from each other, time intervals, marked with the same colour code in Fig.3a and Fig.3b: During the first interval the restored member behaves as a single structural element and the opening of the fault is negligible without any differentiation between the level (distance from the lower edge of the epistyle) at which the opening was measured by the DIC system. In the second interval considerable differences are recorded for the opening of the fault at the levels where each reinforcing pair is placed and the opening of the fault increases at an increasing rate. During the third interval the opening starts increasing quite rapidly until the instant of the local fracture of one of the epistyles corners, which results in an abrupt drop of the load imposed. Finally, during the fourth region the load "recovers" and increases further until the instant of rapid fracture of all the restoration bars. The epistyle's response during the first interval is pretty well attributed to the response of the cement paste layer that was interposed between the faces of the two fragments to enhance their contact. In the second interval the action of the cement layer is eliminated and any additional load is undertaken exclusively by the reinforcing bars either elastically or plastically, depending on the position of each layer. Concerning the third interval, characterized as critical in Fig.3b, it is assumed that the distance between the fragments increases rapidly due to slippage

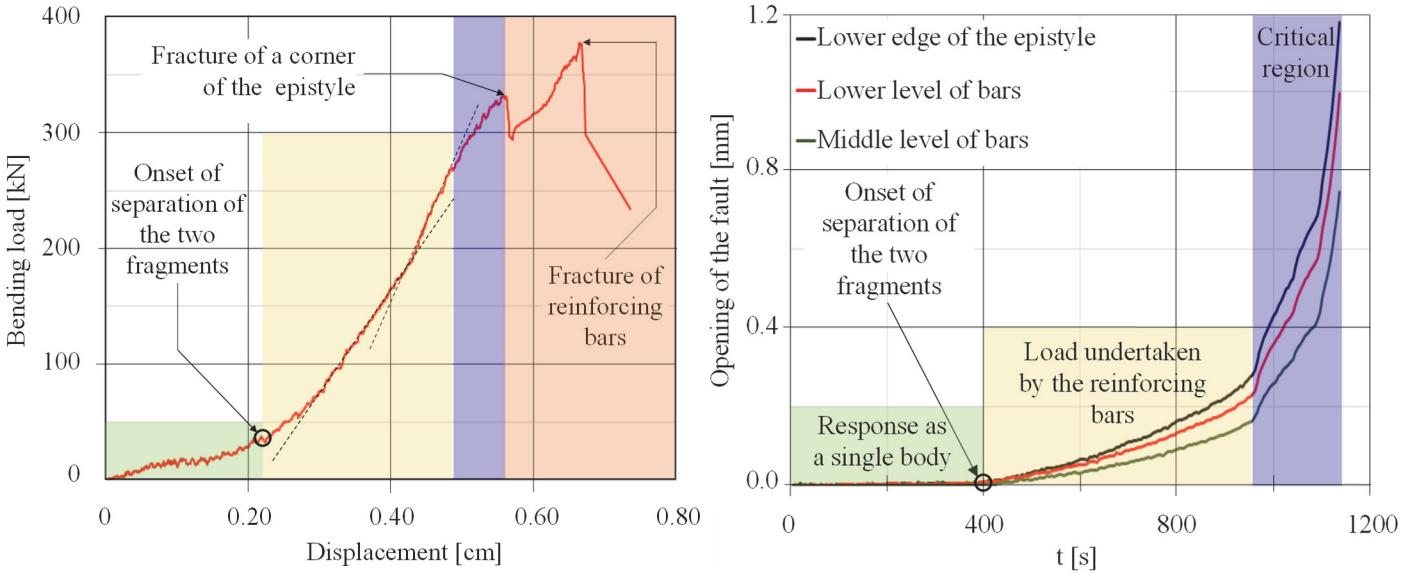

(a) (b)

Figure 3: (a) The bending load versus the displacement (deflection of the epistyle's central cross section); (b) The temporal evolution of distance between the two fragments, at various heights, until the instant of local fracture of one of the epistyle's corners.

(i.e., pull-out) of the restoring bars (and of the cement layer surrounding them) from the body of the marble. As a result, the structure starts behaving as a mechanism and the two fragments exhibit a rotation tendency around the upper line of contact of the two fragments. Therefore, significantly increased compressive loads are exerted at the specific region, leading finally to abrupt fracture of the upper corner of the left fragment (see Fig.2c). From this instant on the stress field is re-distributed rather arbitrarily until the instant of fracture of the reinforcing bars.

Shear loading of mutually interconnected marble epistyles

Again, all specimens of this second protocol were prepared and cured (in-situ) by experienced technicians of the Parthenon Temple work-site. They consisted of two blocks of marble (the first one of cubic shape and the second one of "T"-shape), which were joined together by means of either "I"- or "II"-shaped connectors made of titanium, as it is seen in Fig.4a. The geometry and the dimensions of a typical specimen of this protocol with a "II"-shaped connector is shown in Fig.4b. Grooves (of the shape of the connector) were sculptured on both blocks. Then the connectors were placed in the groove and it was either completely (for the case of the "I"-shaped connector) or partially (for the case of the "II"-shaped connector) covered with a proper cement mortar.

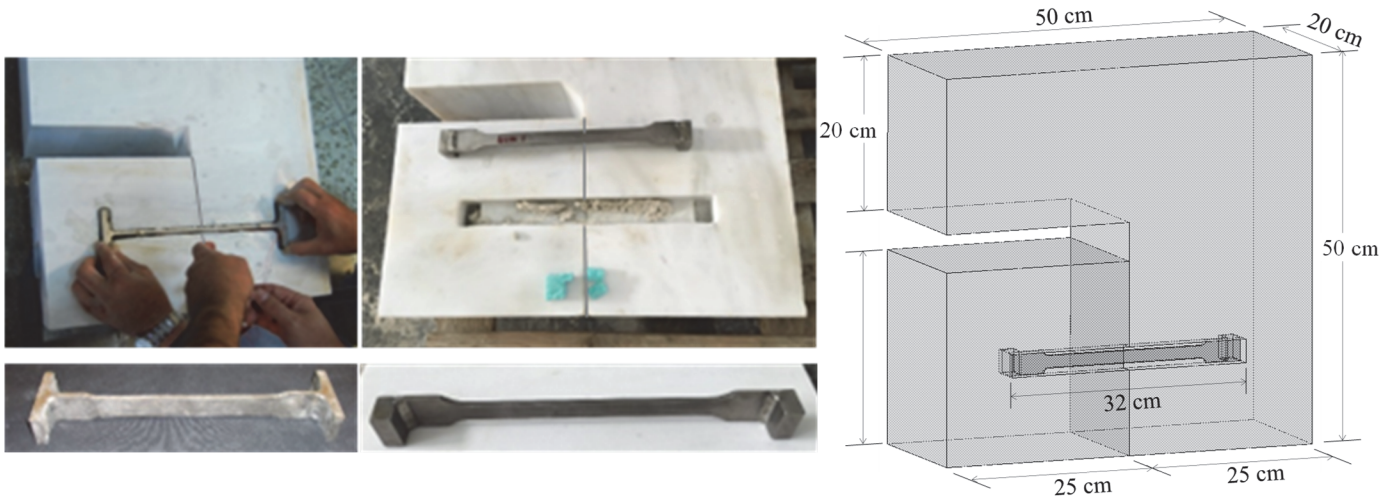

(a) (b)

Figure 4: (a) Typical specimens to be loaded under shear. Connection is achieved by either an "I"-shaped connector (left) or by a "II"-shaped one (right); (b) The geometry and dimensions of the two interconnected blocks forming the "specimens".

The extent of covering of the connector is proven quite crucial for the overall mechanical response of the specimens. In case the connector is fully covered the connections exhibit a very "brittle" response, while, on the other hand, leaving part of the connector uncovered (usually denoted as "relieving space"), at the interface of the interconnected members, offers increased "deformability" to the system [27]. Again, the specimens were cured for one month and then they were tested using an INSTRON servo-hydraulic loading frame the capacity of which was equal to 250 kN. The immobilization of the specimens and the application of the shear load were achieved by means of a specially improvised system. It consisted of metallic rods passing through holes drilled on the "I"-shaped block, at positions which were determined according to the experience of preliminary protocols (preventing local fracture of the blocks in the immediate vicinity of the holes and permitting parallel motion of the "I"-shaped block with respect to the cubic one) and metallic plates. Additional rods were used to immobilize the cubic block on the platform of the frame.

The loading scheme was, again, monotonic, until either the fracture of one of the marble blocks or excessive distortion of the metallic connector. Displacement-controlled conditions were adopted, at a constant of 0.2 mm/min (a rate ensuring a quasi-static loading protocol). A typical specimen with "I"-shaped connector just after it was immobilized on the loading frame is shown in Fig.5a. A close view of a specimen with "II"-shaped connector while prepared to be loaded and, also, while it is being loaded is shown in Figs.5b and 5c, respectively.

The acoustic activity was, again, detected and recorded using eight acoustic sensors (of the R15α type, Mistras Group, Inc., New Jersey, USA). The sensors were properly attached (on both marble blocks) at points of critical importance, on the front- (Fig.5), the rear- and the lateral surfaces of the specimens. The distance between the two blocks was measured by two clip gauges (which were attached at the rear face of the specimens) and, also, by means of the 3D-DIC system (at the front surface). Typical fractured specimens can be seen in Figs.5(d,e).

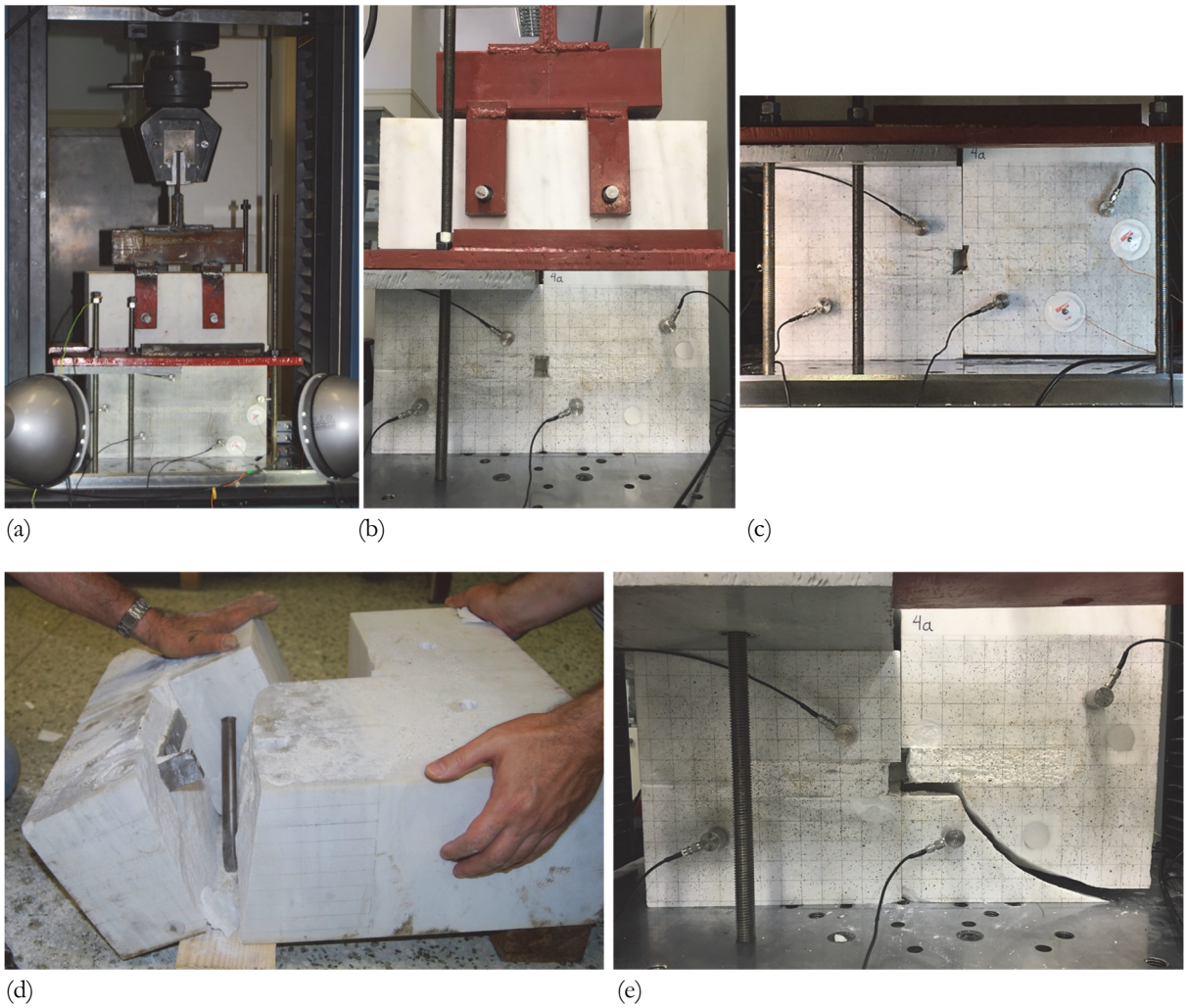

(a) (b) (c)

(d) (e)

Figure 5: (a) Typical specimen with "I"-shaped connector while loaded (a); Detailed view of a specimen with "II"-shaped connector at the onset of loading (b) and just before fracture (c); Fractured specimens with "I"- (d) and "II"-shaped connectors (e).

The response of two characteristic specimens is seen in Fig.6a, in which the applied load is plotted versus the displacement for: (a) a specimen for which the two marble blocks are interconnected using a connector of "I"-shape which is completely covered with cement mortar (denoted as "I"-CC), and, (b) a specimen for which the two blocks are interconnected with a "Π"-shaped connector, partially covered with cement mortar (i.e., a specimen with "relieving space", denoted as "Π"-PC).

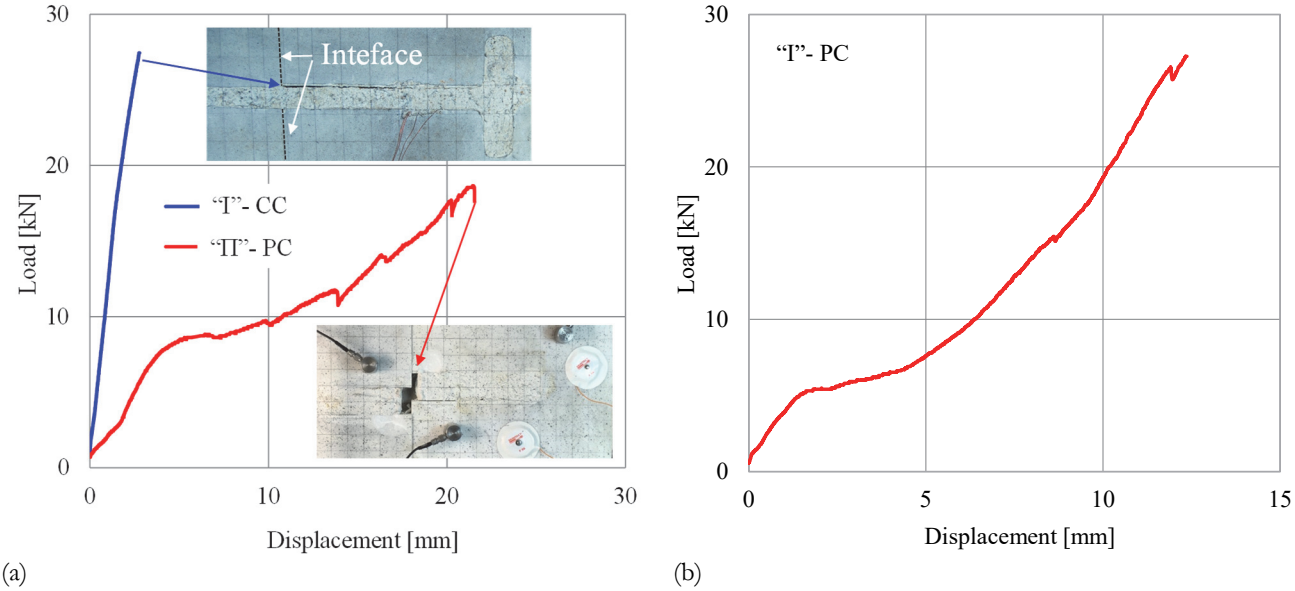

Figure 6: The applied load against the respective displacement: (a) For a specimen with a completely covered "I"-shaped connector ("I"-CC) and for a specimen with a partially covered "Π"-shaped connector ("Π"-PC). Close views of failed specimens are shown in the embedded photos, highlighting the differences in the deformation mechanisms. (b) For a specimen with a partially covered "I"-shaped connector ("I"-PC) [26].

The most striking conclusion deduced from Fig.6a is the huge difference between the two specimens concerning their deformability. Indeed the "relieving space" of the "Π"-PC specimen renders the relative "translation" of the two blocks quite easier since the ductile metallic connector is freely distorted. On the contrary, for the completely covered connector, any shear distortion is prohibited and, therefore, the load is transferred in the form of compression to the cement layer interposed between the titanium connector and the marble blocks and between the two marble blocks themselves. The response of the latter class of specimens is almost perfectly linear (Fig.6a, blue line), reflecting mainly the linear nature of the brittle cement layer, since the metallic connector cannot be deformed freely and therefore it remains in its linear region of response for the major part of loading. On the other hand, the quite "complex" response of the "Π"-PC specimen, (Fig.6a, red line) reflects the different deformation mechanisms activated, including mainly the serious shear deformation (initially elastic and then plastic) of the connector and secondary the compression of the cement layer and the marble blocks. It is interesting to observe the response of a specimen of identical geometry to the one studied here (and under the same loading scheme), the two blocks of which are connected with a partially covered "I"-shaped connector (encoded as "I"-PC), shown in Fig.6b. The similarity with the "Π"-PC specimen is obvious, suggesting that the shape of the connector influences the ultimate load sustained, however the sequence of the mechanisms activated are not seriously affected.

ANALYSIS OF THE EXPERIMENTAL RESULTS USING THE CONCEPTS OF NESM

Bending of an asymmetrically fractured and restored epistyle

During this experiment, the number of acoustic events recorded was N=1038. It was decided to divide them into k=10 groups as follows: The first group contained the first n=200 acoustic events. To obtain the second group a "sliding window" procedure was adopted with the sliding step being equal to n/2=100 acoustic events. Therefore, the second group contained 200 acoustic events starting from the 101st up to the 300th one and so on. Obviously, the 10th group contained only 138 acoustic events (namely from the 901st up to the 1038th one).

As a first step of the analysis, the time parameter τ was determined, for each one of the k=10 groups, as the average of the n time intervals at which each one of the events of this group was recorded. Then, the numerical values of the Cumulative

Distribution Function, $P(>\delta\tau)$, were calculated and plotted versus the respective IT intervals, $\delta\tau$. The $(P(>\delta\tau), \delta\tau)$ curve of each group is then numerically fitted by means of Eqn.(8) (as it was shown as an example in Fig.1). In this way, k=10 numerical values were determined for q and β_q. As a last step, the average frequency of generation of events, as it is quantified by the F-function [28-31], was determined for each one of the k groups, as:

$$F = \frac{1}{\overline{\delta\tau}} \tag{11}$$

where $\overline{\delta\tau}$ denotes the average of the n IT of the events in each group.
It should be highlighted here that combination of Eqn.(11) with Eqn.(9) yields an interesting relation between the F-function and the entropic parameter β_q in terms of the entropic index q as:

$$F = \beta_q \cdot \frac{(q-1)^2}{B\left(2, \frac{2-q}{q-1}\right)} \tag{12}$$

In case $q \to 1$ (i.e., assuming that the phenomena considered are described by Boltzmann-Gibbs Statistical Mechanics) it is obtained that $F=\beta_q$. On the other hand, for phenomena characterized by sub-additivity (i.e., for q>1, as it is the case of the experiments that will be considered in the present study), for example, for q=1.5 then $F=0.5\beta_q$.
Further details about the temporal evolution of q, are obtained from Fig.7, in which q is plotted in terms of the average time τ, in juxtaposition to the temporal evolution of the applied load. It is noticed that q is systematically higher than unity. In others words, the system (complex of marble, titanium and cement paste) is characterized by sub-additivity (recall that for systems with sub-additivity their entropy is smaller compared to the sum of entropies of the constituent sub-systems). Regarding its numerical values, Fig.7 indicates that during the early stages of the loading procedure (namely, for the first group of acoustic events) q attains increased values, equal to $q \approx 1.58$. It is thus concluded that during these early stages the mechanisms of damage, which are activated within the loaded epistyle, are characterized by quite increased organization level (especially for homogeneous materials, this behaviour could be translated to high organization level of the processes responsible for the generation and development of networks of micro-cracks all over the loaded specimen, without significant deviations from a kind of spatially uniform generation of sources of acoustic events).

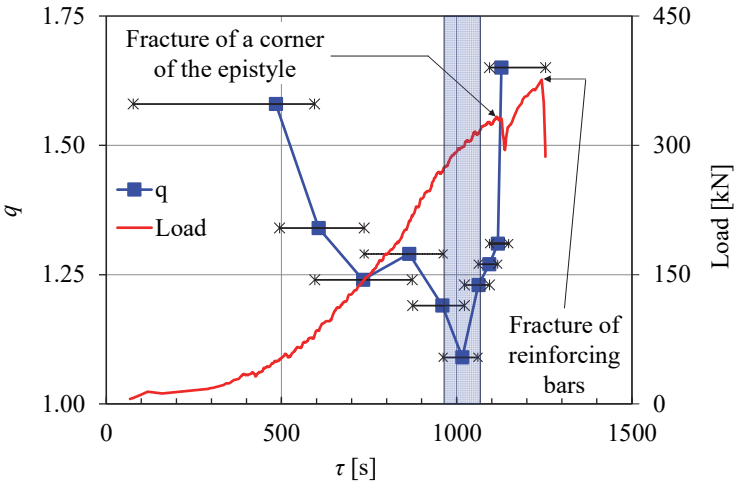

Figure 7: Temporal evolution of q, in juxtaposition to that of the applied load.

Gradually, and while the load increases towards its local maximum (equal to about L=320 kN, attained at τ=1145 s), the value of the entropic index decreases, tending to a minimum (global minimum), which is equal to q=1.09. According to the basic principles of NESM, this, almost systematic, decrease of the q-values towards the critical limit of q=1, is a clear hint that the individual constituent sub-systems, which are formed at the interior of the principal system (in this case the restored epistyle), are now characterized by a decreasing degree of mutual interaction. Moreover, as q tends to the limit of q=1, the mechanisms of damage, which are activated within the structure under load, are characterized by a gradually decreasing organization. In other words, the damage mechanisms are not activated uniformly all over the system but rather areas of

strong concentration of damage nuclei are formed (areas of intense generation and coalescence of micro-cracks), areas at which macroscopic fracture is impending. The latter is well supported by observations [32] according to which for strongly inhomogeneous materials, q-values tending to one indicate generation of an extensive network of cracks.
Focusing again on the response of the epistyle under study it is confirmed that the minimum value of q, which is attained at $\tau \approx 1060$ s, provides a clear warning signal about an upcoming macro-fracture, which was indeed observed about 70 s later (at $\tau \approx 1130$ s), in the form of local fracture of a corner of one of the two restored fragments. From this instant on, the value of q increases again quite rapidly attaining a level equal to q=1.61, reflecting the sudden relief of the stress field due to the abrupt load decrease caused by the local macro-fracture. It would be interesting to further enlighten the interval after the load starts recovering, however for this to be achieved an increased number of groups of acoustic events should be employed. In any case, assuming that the instant of criticality is the fracture of the epistyle (even though it was local) it can be concluded that the decreasing trend of q towards values approaching unit may be considered as an interesting signal (warning relatively early) for impending catastrophic fracture.
Concerning the entropic parameter β_q and the average frequency, F, of production of acoustic events, their temporal evolution is plotted in Fig.8, again, in comparison to the respective evolution of the applied load. It is interesting to observe that, in the criticality region (as it was determined with the aid of the evolution of q), both quantities start increasing rapidly, while before this region their variations were almost negligible, for both β_q and F. This rapid increase tendency is terminated at the instant of fracture of the fragment's corner, reflecting again the instantaneous relief of the stress field.

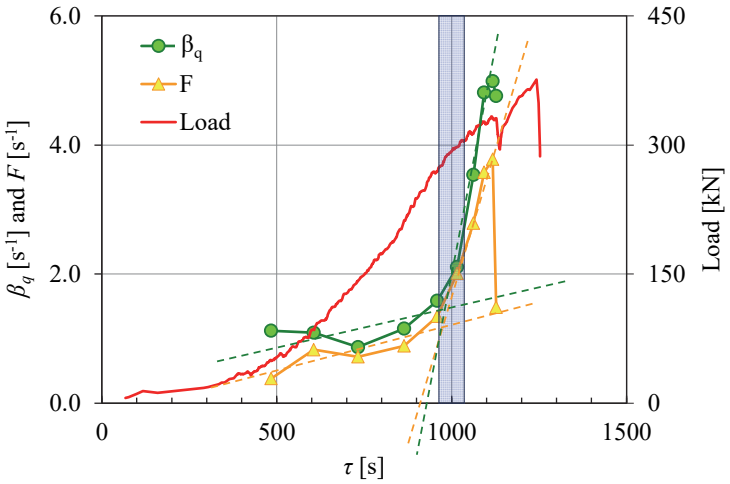

Figure 8: The temporal variation of the entropic parameter β_q and of the average frequency of generation of acoustic events in juxta-position to the respective evolution of the load applied.

Shear loading of mutually interconnected marble epistyles: Specimen with completely covered "T"-shaped connector

During this experiment, the number of acoustic events recorded was N=1091. They were divided into k=9 groups. The first group included the first n=220 successive acoustic events. The second group was obtained by means of the "sliding window" procedure described previously, with the sliding step being now equal to n/2=110 acoustic events. Therefore, the second group contained 220 acoustic events starting from the 111th up to the 330th one and so on. As a result, the 9th group contained only 211 events (from the 880th up to the 1091st one). Adopting the procedure for exploring the acoustic activity using IT intervals and NESM (as it was applied while studying the bending of the asymmetrically fractured and restored epistyle) the k values of q, β_q and those of the mean frequency of generation of acoustic events, F, were determined.
The temporal variation of the entropic index q is plotted in Fig.9 against the average time τ, in comparison to the respective evolution of the applied load. It can be seen from this Fig.9 that the loading procedure is divided into three regions, according to the changes of slope of the load-time plot. In the first region, covering the $0 \text{ s} < \tau < 430$ s interval, the load applied is undertaken elastically by the titanium connector, while the cement layer is compressed between the connector and the marble. The field of stresses that is developed in the marble blocks is quite low compared to its critical limits. In the second region, covering the $430 \text{ s} < \tau < 700$ s interval, the connector has failed and entered into its hardening regime undertaking the additional load inelastically, while the cement layer is still under intense compression. Finally, in the third region, covering the $700 \text{ s} < \tau < 875$ s interval, the load applied causes intense micro-cracking, also, within the marble blocks. In this context, it is concluded (taking into account, also, the spatial distribution of the sources of the acoustic events, as provided by the system of the eight acoustic sensors) that the acoustic activity in the first two regions is attributed to diffuse micro-cracking of the layer of cement paste, while in the third region the acoustic activity is enhanced due to intense micro-

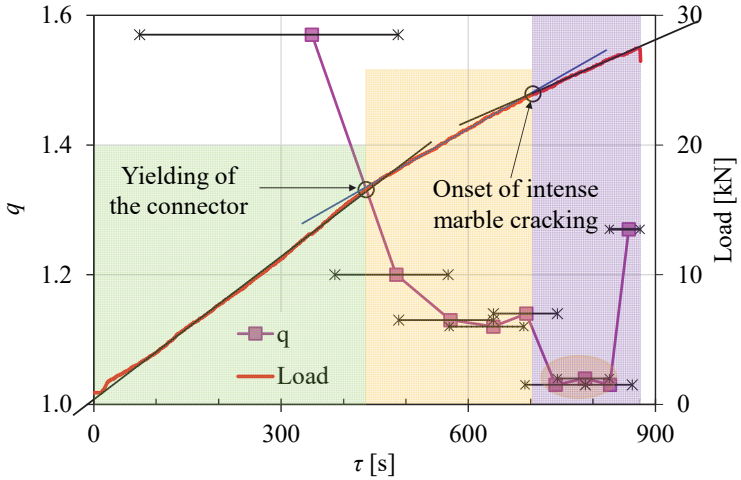

Figure 9: The temporal evolution of q in comparison with the respective one of the applied load, for the shear loading of a specimen with a completely covered "I"-shaped connector.

cracking also of the marble blocks (the latter, however is not diffused, but rather it starts being accumulated in the vicinity of the corners of the connector's flange in the moving marble block, i.e. the "I"-shaped one).

The above argumentation is clearly reflected in the temporal evolution of q. At early loading stages, covering, in fact, the first region of the loading procedure, q attains high values of the order of q=1.57, indicating the existence of sub-systems (in this case the cement layers), within which organized processes of generation of networks of micro-cracks appear. Gradually, q decreases, attaining a global minimum, equal to about q≈1.03, quite close to the critical limit of q=1. It is thus indicated that at these loading levels processes of intense coalescence of the networks of micro-cracks have started, leading eventually to macroscopic fracture. Therefore, it can be said that at the instant τ≈700 s the loaded system is almost ready to enter into its critical stage, namely, that of impending catastrophic fracture.

The temporal evolution of the entropic parameter β_q and that of the average frequency, F, of production of acoustic events which is plotted in next Fig.10 (in comparison with the respective temporal evolution of the applied load) supports the conclusions drawn. Indeed, after the instant τ≈700 s the acoustic activity becomes much more intense up to the instant of fracture of the moving marble block (see Fig.5c), providing an additional index that the system under consideration has now entered into the stage of impending macroscopic fracture.

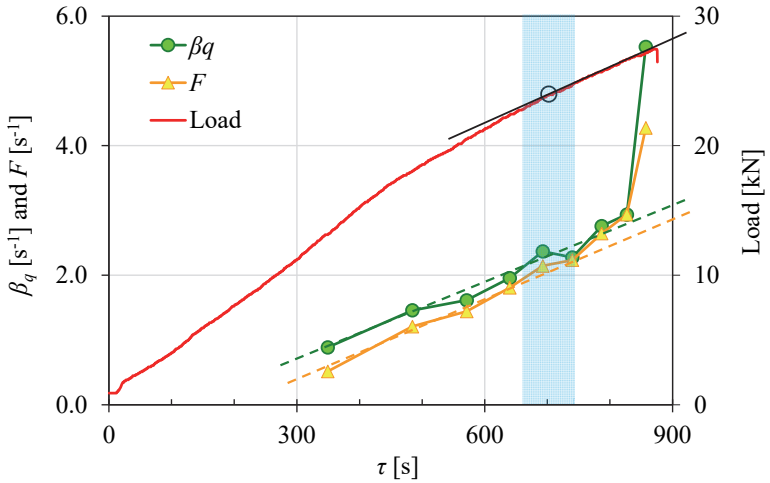

Figure 10: Temporal variation of β_q, and that of the average frequency, F, of production of acoustic events, in comparison with the respective one of the applied load, for shear loading of a specimen with completely covered "I"-shaped connector.

Shear loading of mutually interconnected marble epistyles: Specimen with partially covered "TI"-shaped connector

Taking into account the complicated response of the specific class of specimens, it was deemed necessary to take advantage of additional data (in this case the data obtained by the DIC system), in order to understand the sequence of mechanisms activated. In this direction the horizontal displacement of some strategic points of the movable block (the "I"-shaped one)

(see Fig.11a) was determined. The horizontal displacement of point 2 is plotted in Fig.11b and the respective ones of points 3 and 4 are plotted in Fig.11c. It is seen that up to about 2200 s the horizontal displacement of point 2 is almost zero. In other words, the "T"-shaped block moves almost vertically (parallel to the load direction) and the load is undertaken by the metallic connector, which due to its distortion starts compressing the cement paste layer.

Similar conclusions can be obtained from the horizontal displacement of points 3 and 4, which are of opposite sign (Fig.11c), indicating that while being settled, the movable block exhibits initially a clockwise rotation tendency and then it moves vertically upwards. After the instant t≈2200 s, the "T"-shaped block starts moving, also, horizontally, obviously due to the excessive yielding of the connector and the fragmentation of the cement layer. Therefore, the inclination of the load-displacement plot is significantly reduced (see Fig.6a). Diversifications are observed at about t≈5500 s, an instant at which the horizontal displacement of point 2 starts increasing rapidly after a period that it was stabilized, and the same is true for the horizontal displacements of points 3 and 4

Considering, in addition, the difference between the displacements along the vertical direction of points 1 and 2 (located on either side of the connector), which is drawn in Fig.11d, it is seen that at about t≈5500 s this difference starts increasing rapidly, indicating that the cement layer is decomposed from the marble block (see Figs.5d and 11a) and soon afterwards at about t≈6100 s the specific difference starts increasing quite abruptly indicating that the block is about to be fractured into two parts, as it finally happened at t≈6590 s. Recapitulating, the loading procedure for the specific class of specimens, can be roughly divided into three distinct regions, i.e., 0 s <t< 2200 s, 2200 s <t< 5500 s and 5500 s<t< 6590 s.

The number of acoustic events recorded during this test is equal to N=21422, impressively increased compared to the previous tests discussed (well attributed to the much longer duration of the specific experiment which approaches 6500 s). The acoustic events were divided into k=22 groups. Each group (excluding the last one) contained n=1000 acoustic events. Then, following the procedure for exploration the acoustic activity using the IT intervals and NESM (as it was applied for the study of the asymmetrically fractured and restored epistyle) the numerical values of τ, q, β_q and F were determined for the k=22 groups.

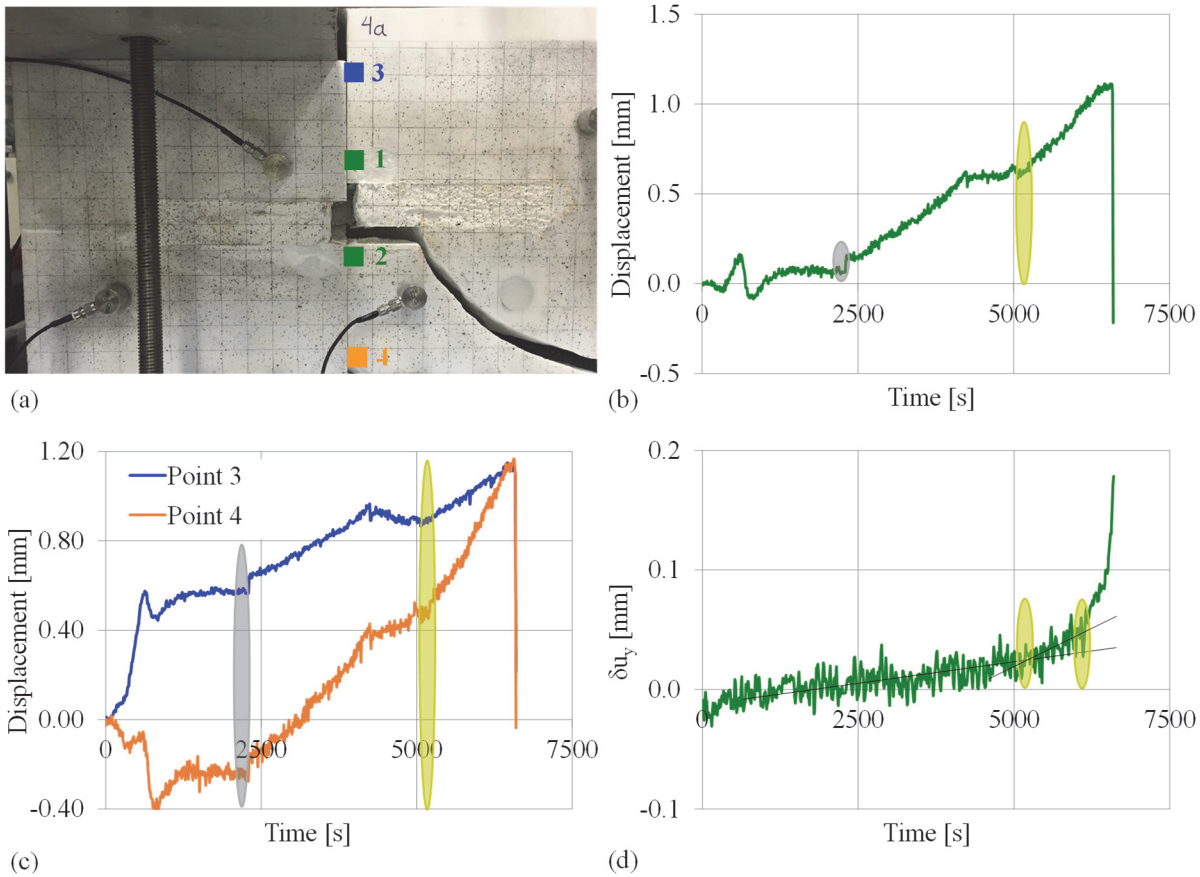

Figure 11: (a) A close view of the area in the vicinity of the interfacial line of the two blocks of marble and the points considered in the analysis; (b) The horizontal displacement of point 2; (c) The horizontal displacement of points 3 and 4; (d) The difference of the displacements along the vertical direction of points 1 and 2.

The temporal evolution of q versus τ is plotted in Fig.12, in juxtaposition to that of the applied load. It is seen, that initially, q attains high values, starting from a level equal to about q=1.50, in good accordance with the initial values of q determined in the previous two protocols. Gradually the values of q decrease towards the critical limit of unity. A first local minimum, equal to q=1.07, is attained at τ≈1900 s. Then, the decreasing trend of q is temporarily interrupted until τ≈2200 s, i.e., the instant at which the "Γ"-shaped block starts moving, also, horizontally, due to yielding of the connector and fragmentation of the cement layer (designated by the reduced slope of the load-displacement plot). After attaining the global minimum value q≈1.04 (at τ≈2500 s), q starts increasing again, almost linearly. It attains a local maximum value, equal to about q≈1.21, at τ≈5300 s (recall that this instant corresponds to the instant at which the difference between the displacements of points 1 and 2 along the vertical direction starts increasing quite rapidly, as it was seen in Fig.11d). Ignoring quantitative details, it is interesting to observe that at both time instants, at which changes in the interaction between the constituent parts of the specimen were indicated by the DIC system, the entropic index q approaches the critical limit of unity.

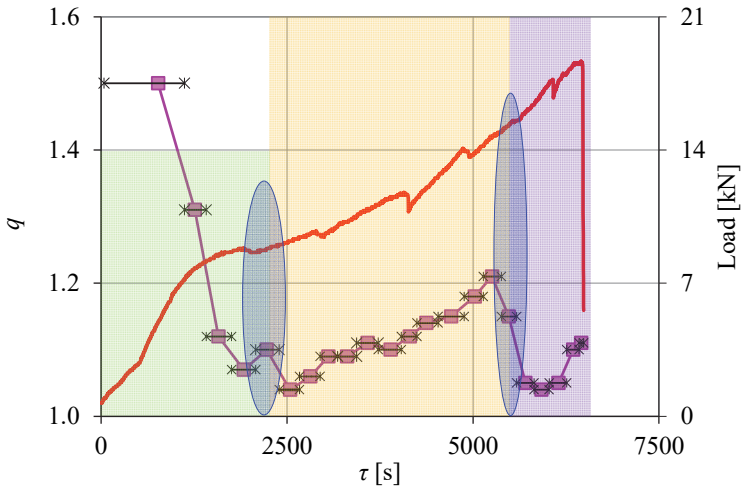

Figure 12: The temporal evolution of q in juxtaposition to that of the applied load for the shear loading of a specimen with a partially covered "Π"-shaped connector.

As a next step, the temporal variation of the acoustic activity is considered in terms of the entropic parameter β_q and the average frequency of production of acoustic events F. In Fig.13 both β_q and F are plotted versus τ, together with the applied load. It can be observed that the acoustic is intensified smoothly (however, with strong local fluctuations) almost during the whole loading procedure, excluding the very last interval (i.e., the 5200 s<τ<6590 s one) during which it starts increasing according to a steeper manner. The fact that the acoustic activity appears intense from very early loading stages is well attributed to both shear effects (namely the friction developed between the two blocks of marble) and, also, to the micro-cracking of the cement layer that is squeezed between the connector and the marble bodies.

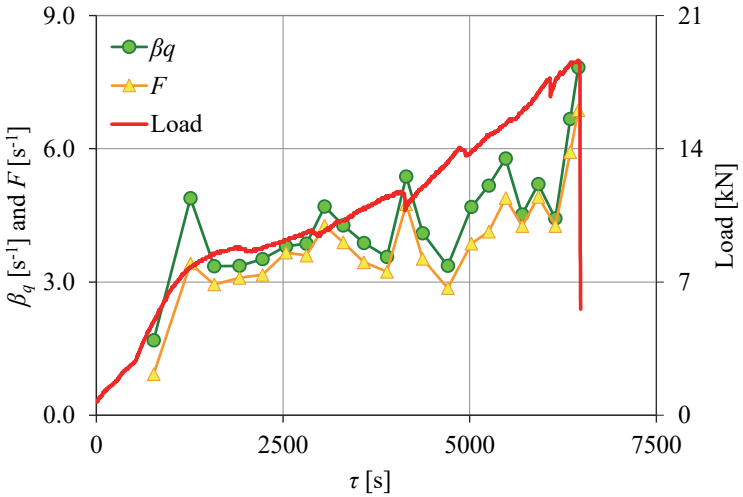

Figure 13: The temporal variation of the entropic parameter, β_q, and of the average frequency, F, of production of acoustic events, in juxtaposition to that of the applied load for the shear loading of a specimen with partially covered "Π"-shaped connector.

DISCUSSION AND CONCLUSIONS

In the present work, the acoustic activity that was developed in two quite different types of marble structures (from the geometrical and the loading points of view) was analyzed, taking advantage of concepts based on the NESM, aiming mainly to detect possible pre-failure indicators. The specific approach, i.e., the analysis of the temporal evolution of the acoustic activity using NESM concepts has been already adopted by the authors' team for the data obtained from previously published experimental protocols, in which homogeneous specimens were tested under various loading schemes [6, 8].
In ref.[6] Dionysos marble plates (a marble variety with remarkably high homogeneity [33-35]) were submitted to direct tension while in ref.[8] Dionysos marble beams were submitted to three-point bending. The analysis of the acoustic activity using NESM concepts revealed that at the initial load stages the entropic index q attains values very close to the critical limit of unity. As the load increased, the entropic index increased, also, approaching a global maximum in the area of $1.35<q<1.41$. This maximum value of q was attained either at the instant of load maximization or very slightly before this landmark instant. From this instant on, q started decreasing until the disintegration of the specimen. This response is reflected in Fig.14, in which the temporal variation of the entropic index is plotted versus the "time-to-failure" parameter, t_f-t (t_f is the time instant of the specimen's fracture), for a notched beam made of Dionysos marble under three-point bending (Fig.14a) and for a double edge-notched Dionysos marble plate under direct tension (Fig.14b).

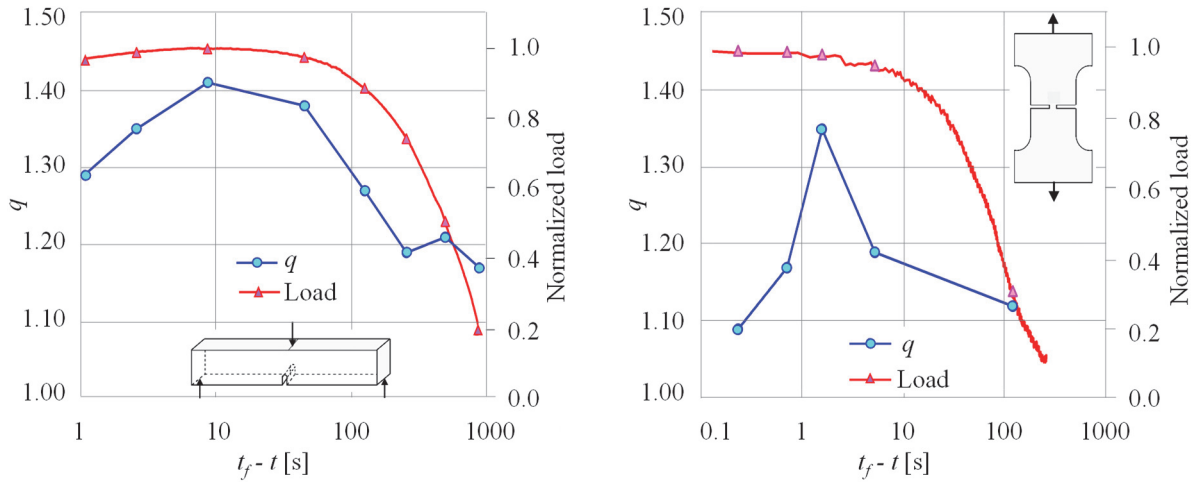

Figure 14: The entropic index and the applied load versus time-to-failure, for notched marble specimens (a) under three-point bending [8], and (b) under uniaxial tension [6].

For the first configuration q is maximized about 10 s before fracture while in the second one the maximization of q is observed about 2 s before macroscopic fracture. Thus, it can be said that the increased homogeneity of the loaded specimen renders description of the initial damage processes more efficient in terms of Boltzmann-Gibbs statistical mechanics, since at the very early loading steps the formation of sub-systems interacting with each other is not as yet achieved. As the load increases, discrete networks of microcracks are developed (enhanced, also, by the presence of the notch, which is a factor prohibiting uniform distribution of the micro-cracks developed) and therefore NESM becomes now more efficient for the analysis and understanding of the process of damage.
Moving away from the almost "perfect" homogeneity of Dionysos marble, concrete beams (either plain or reinforced with metallic fibers) were tested [8]. The beams were loaded under three-point bending. The evolution of the entropic index q in terms of the "time-to-failure" is plotted in Fig.15a (for the plain beams) and in Fig.15b (for the fiber reinforced ones). It is seen that for both cases the entropic index attains quite high values, in the $1.75<q<1.85$ regime, already from very early loading stages. It is thus suggested that the pre-existing material inhomogeneity of the concrete, which is made of aggregates in a cement matrix, enhances the generation of mutually interacting sub-systems already from the beginning of the loading procedure, and, therefore, the description of damage accumulation in terms of the Tsallis entropy rather than in terms of the Boltzmann-Gibbs one, appears imperative.
Besides this quantitative difference of the response of concrete beams (in relation to that of Dionysos marble), another quite interesting feature of the temporal variation of q is deduced from Fig.15b: The numerical values of q start decreasing towards a global minimum value (which is equal to $q\approx1.09$), suggesting that mutually interacting sub-systems of microcracks are gradually substituted by a uniformly distributed network of micro-cracks.

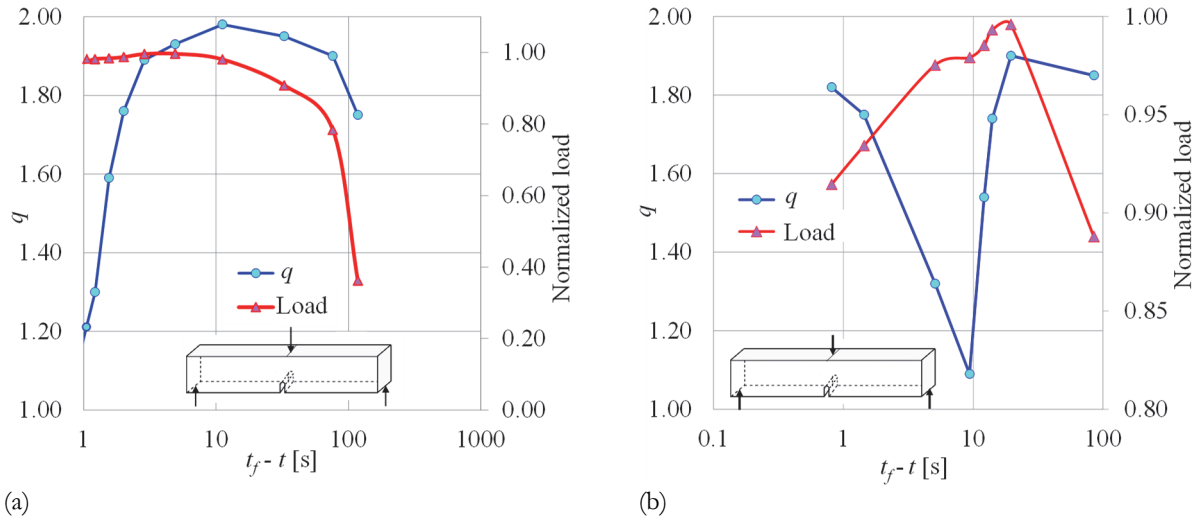

Figure 15: The entropic index and the applied load versus time-to-failure for notched beams made from concrete subjected to three-point bending. (a) Plain beams and (b) Beams reinforced with metallic fibers [8].

However, this decreasing tendency is terminated about 10 s before macroscopic fracture, an instant corresponding to the initiation of fatal propagation of the front of a macro-crack (see ref. [8]) and therefore the damage process ceases being uniform and subsystems of damage nuclei are developed now around the reinforcing fibers located on either side of the propagating front which keep the two fragments in place. As a result, the values of q start increasing again up to the macroscopic fracture of the specimen given that the damage process remains spatially non-uniform.

The specific response of q for the fiber reinforced concrete beam is quite compatible to the one described in the present study: The entropic index attains values well beyond the critical limit of unity (in the very narrow regime of $1.51<q<1.58$) in spite of the quite different systems studied (bending of restored epistyles and shear of two mutually interconnected blocks of marble), indicating that the existence of distinct subsystems (marble blocks, cement layer and metallic bars or connectors) suggests the use of NESM as the optimum tool for the description of damage accumulation. The development of networks of micro-cracks all over the extent of the constituent blocks reduces gradually the non-uniformity of the processes, resulting in a decrease of q towards the limiting value of unity. However, well before the final failure of the composite structure, q starts increasing again as a result of the fact that it entered into its critical stage, namely that of impending fracture, and the consequential development of discrete subsystems within the loaded structure.

Recapitulating, it can be concluded that when the entropic index attains global extremum values the damage processes and the respective damage mechanisms, which are activated within the loaded structure (either of complex nature with pre-existing sub-systems or of homogeneous nature in which the sub-systems are formed and gradually developed), exhibit qualitative changes. In this context, considering the temporal variation of the entropic index in comparison with the respective variation of complementary parameters, which somehow quantify the intensity of the acoustic activity (for example, the frequency of production of acoustic events or the F-function), provides more accurate insight about the level of damage that is accumulated within the loaded structure, or, equivalently, it highlights interesting information concerning its current load carrying capacity, independently of whether it is homogeneous or not.

REFERENCES

[1] Tsallis, C. (1988). Possible generalization of Boltzmann-Gibbs statistics, J. Stat. Phys., 52(1), pp. 479-487. DOI: 10.1007 /bf01016429.

[2] Vallianatos, F., Benson, P., Meredith, P., Sammonds, P. (2012). Experimental evidence of a non-extensive statistical physics behaviour of fracture in triaxially deformed etna basalt using acoustic emissions, EPL, 97(5), 58002. DOI: 10. 1209/0295-5075/97/58002.

[3] Loukidis, A., Triantis, D., Stavrakas, I. (2020). Non-extensive statistical analysis of acoustic emissions recorded in marble and cement mortar specimens under mechanical load until fracture, Entropy, 22(10), 1115. DOI: 10.3390/e22101115.

[4] Vallianatos, F., Michas, G., Papadakis, G. (2018). Nonextensive statistical seismology: An overview. In: T. Chelidze, F. Vallianatos, L. Telesca (Eds.), Complexity of Seismic Time Series: Measurement and Application, Elsevier, Amsterdam, pp. 25-59. DOI: 10.1016/B978-0-12-813138-1.00002-X.

[5] Tsallis, C. (2023). Non-additive entropies and statistical mechanics at the edge of chaos: A bridge between natural and social sciences, Phil. Trans. R. Soc. A, 381(2256), 20220293. DOI: 10.1098/rsta.2022.0293.
[6] Loukidis, A., Triantis, D., Stavrakas, I. (2021). Non-extensive statistical analysis of acoustic emissions: the variability of entropic index q during loading of brittle materials until fracture, Entropy, 23(3), 276. DOI: 10.3390/e23030276.
[7] Tsallis, C. (2004). Nonextensive statistical mechanics: construction and physical interpretation. In: Gell-Mann, M., Tsallis, C. (Eds.), Nonextensive Entropy – Interdisciplinary Applications, Oxford University Press, New York, pp. 1-53. DOI: 10.1093/oso/9780195159769.003.0006.
[8] Kourkoulis, S.K., Loukidis, A., Pasiou, E.D., Stavrakas, I., Triantis, D. (2023). Response of fiber reinforced concrete while entering into the critical stage: An attempt to detect pre-failure indicators in terms of Non-Extensive Statistical Mechanics, Theor. Appl. Fract. Mech., 123, 103690. DOI: 10.1016/j.tafmec.2022.103690.
[9] Clausius, R. (1867). The mechanical theory of heat. John van Voorst, London.
[10] Klein, J.F. (1910) Physical significance of entropy or of the second law. D Van Nostrand Company, New York
[11] Maxwell, J.C., Rayleigh, L. (1904). Theory of heat. Longmans, Green & Co, London.
[12] Buckingham, E. (1900). An outline of the theory of thermodynamics. Macmillan, New York.
[13] Martin, J.S., Smith, N.A., Francis, C.D. (2013). Removing the entropy from the definition of entropy: clarifying the relationship between evolution, entropy, and the second law of thermodynamics, Evo Edu Outreach, 6(1), 30. DOI: 10.1186/1936-6434-6-30.
[14] Einstein, A. (1909). Zum gegenwärtigen Stand des Strahlungsproblems, Physikalische Zeitschrift, 10, pp. 185-193. In: Stachel, J. (Ed.), The Collected Papers of Albert Einstein, The Swiss Years: Writings, 1900-1909, 2, Princeton University Press, Princeton 1993, pp. 541-553.
[15] Tsallis, C. (2012). Nonadditive entropy S_q and nonextensive statistical mechanics: Applications in geophysics and elsewhere, Acta Geophys., 60, pp. 502-525. DOI: 10.2478/s11600-012-0005-0.
[16] Saltas, V., Vallianatos, F., Triantis, D., Koumoudeli, T., Stavrakas, I. (2019). Non-extensive statistical analysis of acoustic emissions series recorded during the uniaxial compression of brittle rocks, Physica A, 528, 121498. DOI: 10.1016/j. physa.2019.121498.
[17] Saltas, V., Peraki, D., Vallianatos, F. (2019). The use of acoustic emissions technique in the monitoring of fracturing in concrete using soundless chemical demolition agent, Frattura ed Integrità Strutturale, 13(50), pp. 505-516, DOI: 10. 3221/IGF-ESIS.50.42.
[18] Greco, A., Tsallis, C., Rapisarda, A., Pluchino, A., Fichera, G., Contrafatto, L. (2020). Acoustic emissions in compression of building materials: q-statistics enables the anticipation of the breakdown point, Eur. Phys. J. Spec. Top., 229(5), pp. 841-849. DOI: 10.1140/epjst/e2020-800232-7.
[19] Loukidis, A., Stavrakas, I., Triantis, D. (2023). Non-extensive statistical mechanics in acoustic emissions: Detection of upcoming fracture in rock materials, Appl. Sci., 13(5), 3249. DOI: 10.3390/app13053249.
[20] Abramowitz, M., Stegun I.A. (1965). Handbook of mathematical functions with formulas, graphs and mathematical tables. Dover Publications Inc., New York.
[21] Storn, R., Price, K. (1997). Differential evolution – a simple and efficient heuristic for global optimization over continuous spaces, J. Glob. Optim., 11, pp. 341-359. DOI: 10.1023/A:1008202821328
[22] Zambas, C. (1992). Structural repairs to the monuments of the Acropolis-The Parthenon, Proc. Institution of Civil Engineers-Civil Engineering, 92(4), pp. 166-176. DOI: 10.1680/icien.1992.21497.
[23] Tassogiannopoulos, A.G. (1986). A contribution to the study of the properties of structural natural stones of Greece. PhD Thesis, National Technical University of Athens, Greece.
[24] Korres, M., Bouras, Ch. (1983). Study for the Parthenon's restoration. Ministry of Culture, Committee for the Conservation of the Acropolis Monuments, Athens.
[25] Angelides, S. (1976.) Replacement of steel connectors by titanium alloy, The Acropolis: Problems-studies-measures to be taken. In: Proc. 2nd Int. Symp. on the Deterioration of Building Stones, National Technical University of Athens, Athens, pp. 351-352.
[26] Kourkoulis, S.K., Dakanali, I., Pasiou, E.D., Stavrakas, I., Triantis, D. (2017). Acoustic Emissions versus Pressure Stimulated Currents during bending of restored marble epistyles: Preliminary results, Frattura ed Integrità Strutturale, 41, pp. 536-551. DOI: 10.3221/IGF-ESIS.41.64.
[27] Zambas, C. (1994). Study for the restoration of the Parthenon (vol. 3b). Ministry of Culture, Committee for the Conservation of the Acropolis Monuments, Athens.
[28] Triantis, D., Kourkoulis, S.K. (2018). An alternative approach for representing the data provided by the acoustic emission technique, Rock Mech. Rock Eng., 51, pp. 2433-2438. DOI: 10.1007/s00603-018-1494-1.

[29] Zhang, J.-Z., Zhou, X.-P., Zhou, L.-S., Berto, F. (2019). Progressive failure of brittle rocks with non-isometric flaws: Insights from acousto-optic-mechanical (AOM) data, Fatigue Fract. Eng. Mater. Struct., 42(8), pp. 1787-1802. DOI: 10.1111/ffe.13019.

[30] Triantis, D., Pasiou, E.D., Stavrakas, I., Kourkoulis, S.K. (2022). Hidden affinities between electric and acoustic activities in brittle materials at near-fracture load levels, Rock Mech. Rock Eng., 55, pp. 1325-1342. DOI: 10.1007/ s00603-021-02711-9.

[31] Yan, X., Su, H., Ai, L., Soltangharaei, V., Xu, X., Yao, K. (2023). Study on stage characteristics of hydraulic concrete fracture under uniaxial compression using acoustic emission, Nondestr. Test. Eval., DOI: 10.1080/10589759.2023. 2255362.

[32] Picoli, S. Jr, Mendes, R.S., Malarne, L.C., Santos, R.P.B. (2009). q-distributions in complex systems: A brief review, Braz. J. Phys., 39(2A), pp. 468-474. DOI: 10.1590/s0103-97332009000400023.

[33] Exadaktylos, G.E., Vardoulakis, I., Kourkoulis, S.K. (2001). Influence of nonlinearity and double elasticity on flexure of rock beams – II. Characterization of Dionysos marble, Int. J. Solids. Struct., 38(22-23), pp. 4119-4145. DOI: 10. 1016/s0020-7683(00)00252-3.

[34] Triantis, D., Kourkoulis, S.K. (2019). Fracture precursor phenomena in marble specimens under uniaxial compression by means of Acoustic Emission data, Frattura ed Integrità Strutturale, 50, pp. 537-547. DOI: 10.3221/IGF-ESIS.50.45.

[35] Stavrakas, I., Kourkoulis, S.K., Triantis, D. (2019). Damage evolution in marble under uniaxial compression monitored by Pressure Stimulated Currents and Acoustic Emissions, Frattura ed Integrità Strutturale, 50, pp. 573-583. DOI: 10. 3221/IGF-ESIS.50.48.